THE JOURNAL OF PHYSICAL CHEMISTRY Letters

Letter

Cite This: J. Phys. Chem. Lett. 2018, 9, 6978−6984

pubs.acs.org/JPCL

Locating Exceptional Points on Multidimensional Complex-Valued Potential Energy Surfaces

Zsuzsanna Benda* and Thomas-C. Jagau*

Department of Chemistry, University of Munich (LMU), D-81377 Munich, Germany

Supporting Information

ABSTRACT: We present a method for locating non-Hermitian degeneracies, called exceptional points (EPs), and minimum-energy EPs between molecular resonances using the complex absorbing potential equation-of-motion coupled-cluster (CAP-EOM-CC) method. EPs are the complex-valued analogue of conical intersections (CIs) and have a similar impact on nonadiabatic processes between resonances as CIs have on nonradiative transitions between bound states. We demonstrate that the CAP-EOM-CC method in the singles and doubles approximation (CAP-EOM-CCSD) yields crossings of the correct dimensionality. The use of analytic gradients enables applications to multidimensional problems. Results are presented for hydrogen cyanide and chloroethylene, for which the location of the crossings of anionic resonances is crucial for understanding the dissociative electron attachment process.

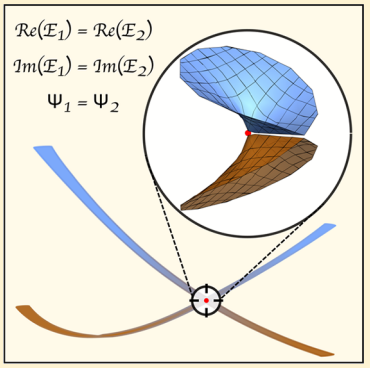

Exceptional points (EPs)[1] are non-Hermitian degeneracies that appear in open quantum systems. They are important in many different fields, such as optics, laser physics, and atomic and molecular physics.[2,3] In this Letter, we investigate molecules that are unstable with respect to electron loss, that is, subject to autoionization.

In the case of autoionizing resonances, EPs have a similar role in deactivation processes as conical intersections (CIs) have in the decay of bound excited states. It is well-known that the interaction of bound electronic states through nuclear motion is often key for understanding processes such as ultrafast decay, isomerization, and photodissociation that are responsible for the photostability of DNA or vision, for example.[4] The probability of a nonadiabatic transition is high near a CI and near an EP as well, and interstate couplings are singular at both types of intersections.[5] EPs are expected to be just as ubiquitous for molecular resonances as CIs are for bound states, but they have been investigated much less.

Linear vibronic coupling (LVC) models were established a long time ago[5,6] for the description of resonance−resonance interactions. The presence of sharp peaks in the vibrational excitation cross section of $H_2 + e^-$ was connected to overlapping resonance states.[7,8] In addition, the interaction of molecular electronic resonances is also important in dissociative electron attachment (DEA), which plays a key role in radiation damage to DNA and in the formation of molecules in interstellar space.[9] We also mention investigations of nonadiabatic effects in resonant Auger decay[10] and interatomic Coulombic decay.[11] However, EPs have been investigated only for a few autoionizing anions: between the $^2A_1$ and $^2B_2$ states of the water anion,[12] and between the $^2A''$ (π^*-type) and $^2A'$ (σ^*_{C-Cl}-type) states of the chloroethylene anion.[6] These investigations were done by scanning the complex-valued potential energy surfaces (CPESs) along a few modes, which requires a large number of calculations and good chemical intuition. In this Letter, we present a method based on analytic gradients for locating EPs on multidimensional CPESs efficiently.

For the time-independent description of autoionizing resonances, as well as for other dissipative systems, we can use non-Hermitian Hamiltonians. Their complex eigenvalues $E = E_R - i\Gamma/2$ give the energy and the decay rate.[13] EPs, where the complex eigenvalues of two states become degenerate, are of special interest because of their importance in nonadiabatic decay, but also because they have properties radically different from Hermitian degeneracies (CIs)[2,14] (see Figure 1). At an EP, not only the eigenvalues but also the eigenvectors coalesce, forming a single self-orthogonal state.[13] The topology of EPs has been confirmed by experiments.[15−20] When encircling a CI, the states do not interchange, but the wave function acquires a geometric phase.[21] In contrast, when encircling an EP, the two states can interchange,[2,22] and the wave function picks up a geometric phase.[23] Encircling the EP in clockwise or in counterclockwise directions yields different final states, which was demonstrated by calculations[24−26] and by experiments on microwave transmission through a waveguide[18] and in an optomechanical system.[19]

The crossing conditions for same-symmetry intersections can be derived in the two-dimensional subspace of the two strongly interacting states. The energy difference between the eigenvalues of the two-dimensional Hamiltonian matrix

Received: October 23, 2018
Accepted: November 27, 2018
Published: November 27, 2018

DOI: 10.1021/acs.jpclett.8b03228
J. Phys. Chem. Lett. 2018, 9, 6978−6984

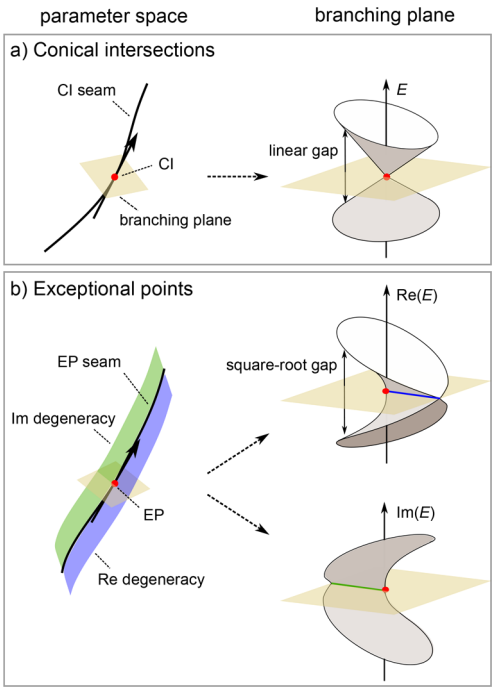

Figure 1. Degeneracy seams in a three-dimensional parameter space and behavior of eigenvalues in the branching plane for (a) Hermitian and (b) non-Hermitian degeneracies.

$$\mathbf{H} = \begin{pmatrix} \epsilon_1 & \omega \\ \omega & \epsilon_2 \end{pmatrix} \tag{1}$$

is $\sqrt{(\epsilon_1 - \epsilon_2)^2 + 4\omega^2}$, where $\epsilon_1 - \epsilon_2$ is the diabatic energy difference and ω is the coupling between the two states. In the case of bound-state crossings, the matrix elements are real, so there are two conditions for degeneracy: $\epsilon_1 - \epsilon_2 = 0$ and $\omega = 0$.[27,28] The eigenvectors remain orthogonal at the CI.

In the case of resonances, ϵ_1, ϵ_2, and ω can be complex; thus, to have an EP between the states, both the real part and the imaginary part of $\sqrt{(\epsilon_1 - \epsilon_2)^2 + 4\omega^2}$ have to be zero.[6,29] This means that the dimensionality of the EP seam is $N - 2$ (where N is the number of nuclear degrees of freedom), just like the CI seam for bound states, but the behavior of the crossing states differs fundamentally between the two cases. The Hamiltonian becomes defective at the EP, the two wave functions coalesce, which means that the eigenvectors no longer span the entire space. In addition, there is one dimension along which the degeneracy of the real parts or that of the imaginary parts can be kept, while the other parts split (Figure 1). The Re and Im degeneracy seams can even form a closed loop containing two EPs, as was demonstrated by Feuerbacher et al.[6] using an LVC model including linear resonance widths and complex coupling terms.

Available methods for locating EPs[30−34] use peculiarities of the EP like the state-exchange phenomenon, the square-root energy gap, or the nonanalytical behavior of energies at the EP. In the method of Cartarius et al.,[31] calculations are performed along closed adiabatic loops, and the interchange of states is used as a sign that the EP is inside the loop. In the iterative three-point and one-point methods of Uzdin and Lefebvre[33] and in the octagon method of Feldmaier et al.,[34] guesses are made for the position of an EP in a two-parameter space utilizing the analytic behavior of the square of the energy difference. Lefebvre and Moiseyev[32] showed that the breakdown of the Padé analytic continuation method can be utilized as well to find EPs.

These methods are most useful for problems with one complex parameter or two real parameters, for example, to describe coalescence in molecular photodissociation, where EPs can arise at specific values of the wavelength and the intensity of the laser.[35] It was suggested that population transfer can be achieved between vibronic states of H_2^+ and Na_2 by a chirped laser pulse, which can be utilized for vibrational cooling.[25,35−38]

In molecules, the number of vibrational degrees of freedom grows quickly with the size of the system ($N = 3N_{atoms} - 6$ for nonlinear molecules), which makes an EP search according to the above-mentioned methods rather complicated. Also, there is an $(N - 2)$-dimensional seam of EPs, from which the most relevant point for estimating the importance of a nonadiabatic process is the minimum-energy EP (MEEP). Here, we present a method for locating EPs and MEEPs within the complex absorbing potential equation-of-motion coupled-cluster (CAP-EOM-CC) formalism[39] by using analytic gradients. This method opens up the possibility of studying DEA in polyatomic systems without the need to impose geometrical constraints.

We employ the CAP-EOM-CC method with a box-type quadratic CAP added at the Hartree−Fock (HF) level as outlined in refs 39 and 40. CAP-EOM-CC provides the two resonances in one calculation if the same set of parameters (CAP strength parameter η and box size parameters r_α^0, $\alpha = x$, y, z) are used for both states,[41] which ensures the balanced description of the crossing states.[9]

The CAP-EOM-CC right wave function of state λ is defined as

$$|\Psi_\lambda) = \hat{R}^\lambda e^{\hat{T}} |\Phi_{HF}) \tag{2}$$

where $\hat{T}$ is the cluster operator and operator $\hat{R}^\lambda$ can be chosen in different forms to create excited, ionized, electron-attached, or spin-flipped states.[42] The scalar product $\langle \phi_i | \phi_j \rangle$ is replaced by the c-product[43] $(\phi_i | \phi_j) \equiv \langle \phi_i^* | \phi_j \rangle$, which yields a complete set of eigenvectors if there is no degeneracy.[13] At EPs, however, the c-norm of the corresponding eigenvector is zero, even though the eigenvector is nonzero (self-orthogonality).[13,43]

It should be mentioned here that truncated CC and EOM-CC methods do not give the correct shape and dimensionality of same-symmetry crossings of bound states.[44−46] This is because truncation introduces non-Hermiticity, which changes the crossing conditions. If we look at the problem as a real nonsymmetric perturbation to a real symmetric matrix, a CI is blown up to a circle of EPs because of the perturbation, and complex eigenvalues appear within the circle.[47]

In the case of a truncated CAP-EOM-CC treatment of resonances, the Hamiltonian is complex non-Hermitian. As every complex matrix is similar to a complex symmetric matrix,[29] the crossing conditions of a complex symmetric H of eq 1 apply, so truncated CAP-EOM-CC is expected to give the correct dimensionality of the crossing seam. We demonstrate this by calculations on the anions of hydrogen cyanide and chloroethylene. Similar to truncated EOM-CC methods, truncated CAP-EOM-CC can be systematically improved toward the CAP-FCI limit by including higher-order excitations.

DOI: 10.1021/acs.jpclett.8b03228
J. Phys. Chem. Lett. 2018, 9, 6978−6984

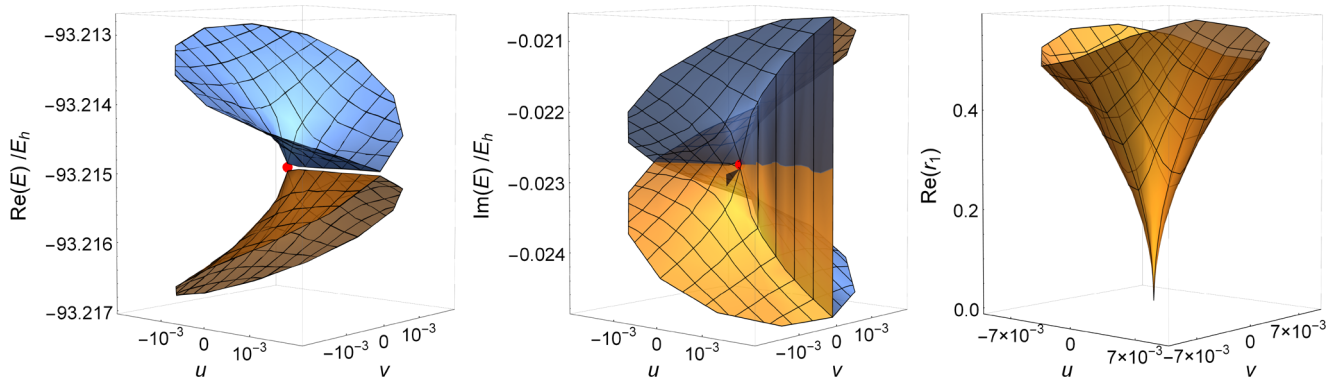

Figure 2. Real and imaginary parts of the CPESs above the branching plane corresponding to the EP at ∠ = 165° from Figure 3 (marked by a red dot here). The third panel shows the real part of the phase rigidity for the first state. For the definition of **u** and **v** vectors, see the Supporting Information. Calculations were performed with the fixed CAP parameters of the EP (see the Supporting Information).

Because of the coalescence of the wave functions at an EP, the wave function amplitudes diverge.[13] The phase rigidity (r_λ)[48−51] is the ratio of the c-norm and the regular norm, and it can be used as an indicator of an EP. Because of the nonsymmetric nature of CAP-EOM-CC we calculate it as

$$r_\lambda = \frac{(\tilde{\Psi}_\lambda|\Psi_\lambda)}{\langle\tilde{\Psi}_\lambda|\Psi_\lambda\rangle} = \frac{A}{A^2+B^2} - i\frac{B}{A^2+B^2} \tag{3}$$

$$A = 1 + 2\sum_i \mathrm{Im}(L_i^\lambda)\,\mathrm{Im}(R_i^\lambda) \tag{4}$$

$$B = 2\sum_i \mathrm{Re}(L_i^\lambda)\,\mathrm{Im}(R_i^\lambda) \tag{5}$$

where $\tilde{\Psi}_\lambda$ is the left CAP-EOM-CC wave function; L_i^λ and R_i^λ are the left and the right EOM amplitudes corresponding to single, double, etc. excitations; and we used the fact that left and right eigenvectors are biorthogonalized using the c-product

$$\mathrm{Re}(\tilde{\Psi}_\lambda|\Psi_\lambda) = \sum_i (\mathrm{Re}(L_i^\lambda)\,\mathrm{Re}(R_i^\lambda) - \mathrm{Im}(L_i^\lambda)\,\mathrm{Im}(R_i^\lambda)) = 1 \tag{6}$$

$$\mathrm{Im}(\tilde{\Psi}_\lambda|\Psi_\lambda) = \sum_i (\mathrm{Re}(L_i^\lambda)\,\mathrm{Im}(R_i^\lambda) + \mathrm{Im}(L_i^\lambda)\,\mathrm{Re}(R_i^\lambda)) = 0 \tag{7}$$

The phase rigidity is complex in our case because of different left and right eigenvectors in truncated CAP-EOM-CC. For well-separated resonances, its value should be close to 1 with a negligible imaginary part, and it should go to 0 as the EP is approached, because the amplitudes and thus the regular scalar product grow. For a full CC expansion, the phase rigidity would have purely real values.

To locate EPs on multidimensional CPESs, we use the fact that both the real and the imaginary energy differences have to go to zero as the EP is approached. The corresponding gradient difference vectors can be used to determine directions in which the energy differences decrease, and a method similar to the direct method by Bearpark et al.[52] for locating crossing points of bound states can be applied.

We use gradient $\tilde{\mathbf{g}}$ to locate any EP between two states

$$\tilde{\mathbf{g}} = \mathbf{f}_{\mathrm{Re}} + \mathbf{f}_{\mathrm{Im}} \tag{8}$$

$$\mathbf{f}_{\mathrm{Re}} = 2(\mathrm{Re}(E_2) - \mathrm{Re}(E_1))\frac{\mathbf{x}_{\mathrm{Re}}}{\|\mathbf{x}_{\mathrm{Re}}\|} \tag{9}$$

$$\mathbf{f}_{\mathrm{Im}} = -4(\mathrm{Im}(E_2) - \mathrm{Im}(E_1))\frac{\mathbf{x}_{\mathrm{Im}}}{\|\mathbf{x}_{\mathrm{Im}}\|} \tag{10}$$

where $\mathbf{x}_{\mathrm{Re}}$ and $\mathbf{x}_{\mathrm{Im}}$ are the gradient difference vectors

$$\mathbf{x}_{\mathrm{Re}} = \mathrm{Re}(\mathbf{G}_2) - \mathrm{Re}(\mathbf{G}_1) \tag{11}$$

$$\mathbf{x}_{\mathrm{Im}} = -2(\mathrm{Im}(\mathbf{G}_2) - \mathrm{Im}(\mathbf{G}_1)) \tag{12}$$

We presented the implementation of $\mathrm{Re}(\mathbf{G})$ in an earlier paper[40] and used it for locating resonance equilibrium structures[53] and for the initial optimization of minimum-energy crossing points (MECPs) between anionic states and their parent neutral states.[54] We complement our implementation with $\mathrm{Im}(\mathbf{G})$ in the current work (see the Supporting Information for the gradient formula).

To find the minimum-energy exceptional point (MEEP), one would additionally have to minimize E_R of one of the states in the subspace orthogonal to the two-dimensional branching plane, as is done for the MECP of bound states.[52] While in the latter case the branching plane is spanned by the gradient difference vector and the nonadiabatic force matrix element $(\mathbf{h})$,[14,55] in the case of EPs the two-dimensional branching plane is spanned by different combinations of the $\mathbf{x}_{\mathrm{Re}}$, $\mathbf{x}_{\mathrm{Im}}$, $\mathbf{h}_{\mathrm{Re}}$, and $\mathbf{h}_{\mathrm{Im}}$ vectors.

In our current implementation, the gradient of the second state is orthogonalized to the plane spanned by $\mathbf{x}_{\mathrm{Re}}$ and $\mathbf{x}_{\mathrm{Im}}$ using projector $\mathcal{P}$

$$\mathbf{g} = \mathcal{P}\mathrm{Re}(\mathbf{G}_2) \tag{13}$$

which is expected to cause slower convergence than orthogonalization to the branching plane, but the calculation of $\mathbf{h}_{\mathrm{Re}}$ and $\mathbf{h}_{\mathrm{Im}}$ is avoided.

The final gradient used for the MEEP optimization is given as

$$\bar{\mathbf{g}} = \mathbf{f}_{\mathrm{Re}} + \mathbf{f}_{\mathrm{Im}} + \mathbf{g} \tag{14}$$

The outlined methods were implemented in Q-Chem,[56] built upon the MECP search implementation by Epifanovsky and Krylov.[57]

To test the EP optimization and MEEP optimization algorithms and to investigate the topology of EPs within the CAP-EOM-CC singles and doubles (CAP-EOM-CCSD) model, we performed calculations on the HCN^- anion,

DOI: 10.1021/acs.jpclett.8b03228
J. Phys. Chem. Lett. 2018, 9, 6978−6984

which can have a one-dimensional EP seam between two resonance states of the same symmetry and multiplicity at bent structures. We looked at crossings between two ^{2}A′ states that correspond to a $^2\Pi$ state and a $^2\Sigma^+$ state in linear geometry and presumably play a part in DEA to HCN.

For these calculations we used the CAP-EOM-EA-CCSD method and the standard Dunning basis set aug-cc-pVTZ augmented with three extra p functions on each atom (following the augmentation scheme described in ref 39). The CAP strength parameter was kept fixed at the value 9×10^{-3} a.u.,[58] but the box size parameters were relaxed during the EP optimization.

First we located EPs at five different constrained bond angles between 155° and 175° using eq 8 for the optimization. To verify the shape of the CPESs around EPs, we investigated the EP corresponding to ∠ = 165°. Because there are just three degrees of freedom for HCN^-, it is simple to determine the branching plane in this case (see the Supporting Information). In Figures 2 and 3 it can be seen that the dimensionality of the

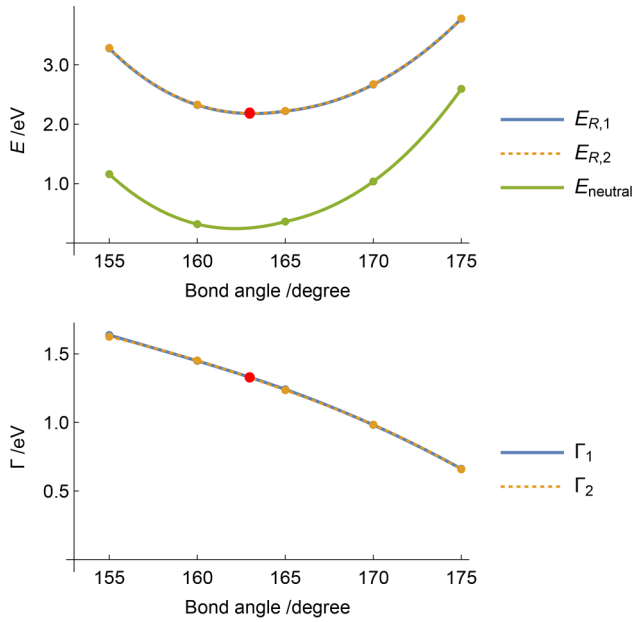

Figure 3. Resonance positions and widths and the energy of the parent neutral state along the EP line of HCN^-. The optimized MEEP is marked by a red dot. Optimized structural parameters and box size parameters are available in the Supporting Information.

EP is correctly described by the CAP-EOM-CCSD method: there is a one-dimensional EP seam, and the degeneracy is lifted in the branching plane, as expected. The real parts of the surfaces remain degenerate in one direction, and the imaginary parts interchange here, while the imaginary parts are degenerate in the opposite direction,[59] which is also in agreement with analytical models.

The real part of the phase rigidity of state 1 is plotted in Figure 2. It is of the order of 10^{-2} at the approximate EP, but it is below 0.6 already at radius 0.01 (approximately 0.007 Å change in the bond lengths). The imaginary part of the phase rigidity is negligible, with values between −0.008 and 0.007 for all points calculated (see the Supporting Information).

The EPs found at different bond angles cover a large range of E_R and Γ values (Figure 3), and the difference between the two states is typically smaller than 6 meV for both quantities (see the Supporting Information). The third-order interpolating functions for $E_{R,1}$ and $E_{R,2}$ have a minimum at ∠ = 163.16° and 163.18°, respectively. The MEEP (shown as a red dot in Figure 3) was converged with a slightly looser threshold than the previous EP points, so the energy difference of the two states is somewhat larger than before (20 meV for E_R and 2 meV for Γ). The need to use looser thresholds is probably due to the fact that $\mathbf{g}$ is not exactly parallel to the EP line. The MEEP has internal coordinates R_{CN} = 1.165 Å, R_{CH} = 1.162 Å, and ∠ = 162.98°, the latter in very good agreement with the above approximated values, which indicates that the looser thresholds do not induce a large error in the structure.

To try out our method for a larger system with more degrees of freedom, we investigated chloroethylene, which is a good model for biologically important halogenated compounds. For example, halogenated DNA bases are used as sensitizers in radiation therapy, and it is believed that DEA involving resonance states plays a role in this process by inducing strand breaks in DNA.[60] Experimental studies of chloro-substituted ethylenes[61−65] suggest that electron attachment produces a π^* resonance, which, through out-of-plane motions, converts to a σ^* state that is dissociative along a C−Cl bond. This DEA process for removing a chloride ion from the molecule might be important in the detoxification of these substances, which are common pollutants of groundwater.[66]

In an earlier paper we presented vertical attachment energies (VAEs) and MECPs between the lowest-energy anionic state and the parent neutral state for chloro-substituted ethylenes.[54] Here, we located the MEEP between the π^* and σ^* states of the chloroethylene anion so that we can construct a complete pathway for DEA. These calculations were carried out using CAP-EOM-EA-CCSD and the aug-cc-pVDZ+3p basis set (3 extra p functions on C and Cl atoms). The two states have different symmetry at planar structures (A″ and A′), which means they cannot interact. At the MEEP, the Cl atom is bent slightly out of the molecular plane; this allows for the interaction of the two states. The C−Cl bond and, to a smaller extent, the C−C bond are elongated compared to the equilibrium structure of the neutral molecule (see the Supporting Information). Feuerbacher et al. also located an EP for this system[6] by changing the C−Cl bond length and the Cl out-of-plane angle in increments and leaving all other coordinates fixed at their value at the neutral equilibrium structure. Our method allows for the efficient optimization of all nuclear coordinates, and in this way it yields the MEEP, which is more relevant for assessing the probability of the DEA process.

To check the shape of the CPESs near the MEEP, we performed calculations in the $\mathbf{x}_{Re}$−$\mathbf{x}_{Im}$ plane. The resulting surfaces (Figure 4) have two EPs in the plane, and the shape formed by the Re(E) and the Im(E) degeneracy seams resembles an ellipse. This is in line with LVC results and ab initio calculations of Feuerbacher et al.,[6] who introduced the term doubly intersecting complex energy surfaces (DICES) for this phenomenon. In Figure 4 the ellipse fitted to the Im(E) surface crossing can be seen. The optimized MEEP is not exactly on the ellipse; differences in bond lengths between the MEEP and the corresponding approximated point on the ellipse, EP_1, are smaller than 0.001 Å. The C−Cl bond at the other EP on the ellipse, EP_2, is shorter by 0.013 Å than at EP_1, and the H−C−C−Cl dihedral angle is −4.1° at EP_2 compared to 2.3° at EP_1 and MEEP.

DOI: 10.1021/acs.jpclett.8b03228
J. Phys. Chem. Lett. 2018, 9, 6978−6984

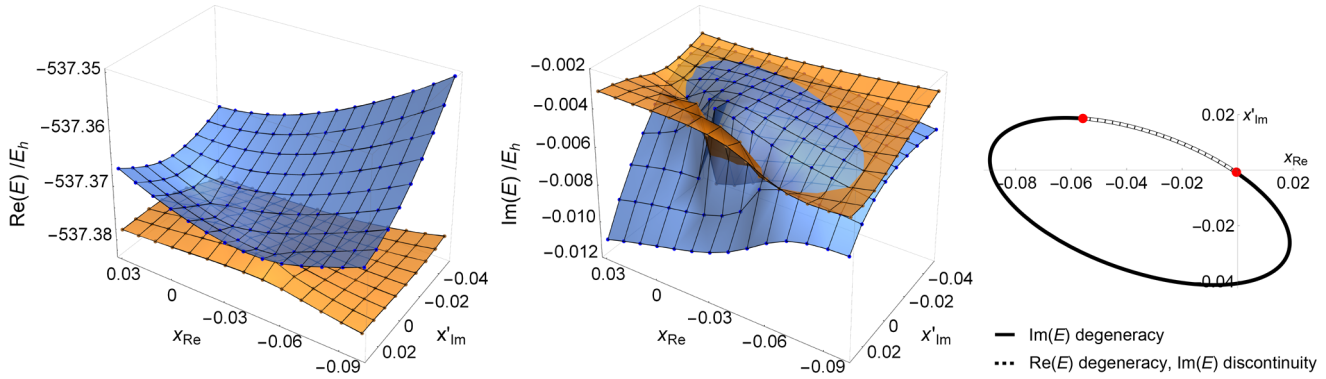

Figure 4. CPESs in the vicinity of the MEEP point (origin) between the π^* and the σ^* states of chloroethylene, plotted above the plane spanned by the real gradient difference vector ($\mathbf{x}_{Re}$) and the imaginary gradient difference vector orthogonalized to $\mathbf{x}_{Re}$ ($\mathbf{x}'_{Im}$). Real and imaginary degeneracy seams form an ellipse (see the Supporting Information for details of the fitting), with two EPs (marked with red dots) separating the real and the imaginary seams. Calculations were done with the fixed CAP parameters of the MEEP (see the Supporting Information).

To construct a pathway for DEA, we performed linear interpolation between the neutral equilibrium structure and the MEEP and between the MEEP and the MECP. The π^* state has a much smaller resonance width than the σ^* state in the Franck−Condon region, but the width of the latter state quickly decreases along the DEA pathway (Figure 5). At the MEEP it is similar to the vertical width of the π^* state. Transition from π^* to σ^* occurs near the MEEP where the coupling of the two states is large. From the MEEP both the position and the width of the σ^* resonance decrease monotonically, until the MECP with the neutral state is reached, and the anionic state becomes stable with respect to electron loss. Note that at the MECP regular EOM-CCSD was used for the calculation of the σ^* state; thus, Γ is zero by definition.

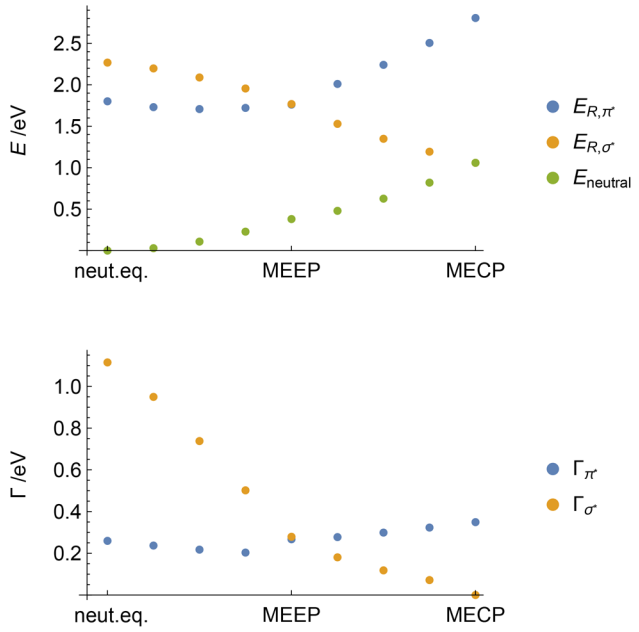

Figure 5. Resonance positions and widths of π^* and σ^* anionic states and energy of the parent neutral state of chloroethylene along the DEA pathway. For π^* and σ^* states, their respective optimal CAP strength parameter[67] was used at each point where possible (parameter values and additional information are given in the Supporting Information).

The MEEP has slightly lower energy (1.761−1.768 eV) than the VAE of the π^* state (1.801 eV[54]), and the MECP is at a substantially lower energy than the previous two (1.059 eV[54]), which means that DEA can proceed along a completely barrier-free route. The long lifetime of the π^* state relative to the σ^* state and the accessibility of the MEEP makes electron attachment to the π^* orbital very likely to produce chloride ions as suggested also by experiments. However, experiments find the maximum of the DEA cross section at around 1.2−1.3 eV,[63,64] that is, at considerably lower energy than our VAE. A similar deviation was obtained and analyzed in more detail in ref 6. We also note that the π^* state has a minimum before reaching the MEEP, which is expected to elongate the time the anion is subject to electron loss. To model how the properties of real and imaginary surfaces influence the efficiency of the DEA process, dynamical simulations of nuclear motion would be needed.

In summary, we presented a method for locating EPs and MEEPs on multidimensional CPESs using analytic gradients. The peculiar shape of CPESs around EPs was discussed, and the ability of the CAP-EOM-CCSD method to correctly describe the vicinity of EPs was demonstrated. DEA to chloroethylene was investigated by locating the MEEP between π^* and σ^* anionic states and constructing a pathway from the neutral equilibrium structure to the σ^*−neutral MECP through the MEEP.

■ ASSOCIATED CONTENT

Supporting Information

The Supporting Information is available free of charge on the ACS Publications website at DOI: 10.1021/acs.jpclett.8b03228.

Complex gradient formula, CAP parameters, structural parameters and energies for optimized points, description of determining the branching plane, and details of fitting (PDF)

■ AUTHOR INFORMATION

Corresponding Authors

*E-mail: zsuzsanna.benda@cup.uni-muenchen.de.
*E-mail: th.jagau@lmu.de.

ORCID

Zsuzsanna Benda: 0000-0002-6714-0337
Thomas-C. Jagau: 0000-0001-5919-424X

DOI: 10.1021/acs.jpclett.8b03228
J. Phys. Chem. Lett. 2018, 9, 6978−6984

Notes

The authors declare no competing financial interest.

■ ACKNOWLEDGMENTS

We thank Professor Anna Krylov, Professor Lorenz Cederbaum, and Professor Nimrod Moiseyev for helpful comments on the manuscript. This work has been supported by the Deutsche Forschungsgemeinschaft through Grant JA 2794/1-1 (Emmy Noether program).

■ REFERENCES

(1) Kato, T. *Perturbation Theory of Linear Operators*; Springer, 1966.
(2) Berry, M. V. Physics of Nonhermitian Degeneracies. *Czech. J. Phys.* **2004**, *54*, 1039−1047.
(3) Heiss, W. D. The physics of exceptional points. *J. Phys. A: Math. Theor.* **2012**, *45*, 444016.
(4) *Conical Intersections: Theory, Computation and Experiment*; Domcke, W., Yarkony, D. R., Köppel, H., Eds.; World Scientific: Singapore, 2011.
(5) Estrada, H.; Cederbaum, L. S.; Domcke, W. Vibronic coupling of short-lived electronic states. *J. Chem. Phys.* **1986**, *84*, 152−169.
(6) Feuerbacher, S.; Sommerfeld, T.; Cederbaum, L. S. Intersections of potential energy surfaces of short-lived states: The complex analogue of conical intersections. *J. Chem. Phys.* **2004**, *120*, 3201−3214.
(7) Narevicius, E.; Moiseyev, N. Fingerprints of Broad Overlapping Resonances in the e + H_2 Cross Section. *Phys. Rev. Lett.* **1998**, *81*, 2221−2224.
(8) Narevicius, E.; Moiseyev, N. Trapping of an Electron due to Molecular Vibrations. *Phys. Rev. Lett.* **2000**, *84*, 1681−1684.
(9) Jagau, T.-C.; Bravaya, K. B.; Krylov, A. I. Extending Quantum Chemistry of Bound States to Electronic Resonances. *Annu. Rev. Phys. Chem.* **2017**, *68*, 525−553.
(10) Cederbaum, L. S.; Chiang, Y.-C.; Demekhin, P. V.; Moiseyev, N. Resonant Auger decay of molecules in intense X-ray laser fields: light-induced strong nonadiabatic effects. *Phys. Rev. Lett.* **2011**, *106*, 123001.
(11) Demekhin, P. V.; Stoychev, S. D.; Kuleff, A. I.; Cederbaum, L. S. Exploring interatomic coulombic decay by free electron lasers. *Phys. Rev. Lett.* **2011**, *107*, 273002.
(12) Haxton, D. J.; Rescigno, T. N.; McCurdy, C. W. Topology of the adiabatic potential energy surfaces for the resonance states of the water anion. *Phys. Rev. A: At., Mol., Opt. Phys.* **2005**, *72*, 022705.
(13) Moiseyev, N. *Non-Hermitian Quantum Mechanics*; Cambridge University Press, 2011.
(14) Yarkony, D. R. Diabolical conical intersections. *Rev. Mod. Phys.* **1996**, *68*, 985−1013.
(15) Dembowski, C.; Gräf, H.-D.; Harney, H. L.; Heine, A.; Heiss, W. D.; Rehfeld, H.; Richter, A. Experimental Observation of the Topological Structure of Exceptional Points. *Phys. Rev. Lett.* **2001**, *86*, 787−790.
(16) Lee, S.-B.; Yang, J.; Moon, S.; Lee, S.-Y.; Shim, J.-B.; Kim, S. W.; Lee, J.-H.; An, K. Observation of an Exceptional Point in a Chaotic Optical Microcavity. *Phys. Rev. Lett.* **2009**, *103*, 134101.
(17) Gao, T.; Estrecho, E.; Bliokh, K. Y.; Liew, T. C. H.; Fraser, M. D.; Brodbeck, S.; Kamp, M.; Schneider, C.; Höfling, S.; Yamamoto, Y.; et al. Observation of non-Hermitian degeneracies in a chaotic exciton-polariton billiard. *Nature* **2015**, *526*, 554.
(18) Doppler, J.; Mailybaev, A. A.; Böhm, J.; Kuhl, U.; Girschik, A.; Libisch, F.; Milburn, T. J.; Rabl, P.; Moiseyev, N.; Rotter, S. Dynamically encircling an exceptional point for asymmetric mode switching. *Nature* **2016**, *537*, 76−79.
(19) Xu, H.; Mason, D.; Jiang, L.; Harris, J. G. E. Topological energy transfer in an optomechanical system with exceptional points. *Nature* **2016**, *537*, 80.
(20) Zhou, H.; Peng, C.; Yoon, Y.; Hsu, C. W.; Nelson, K. A.; Fu, L.; Joannopoulos, J. D.; Soljačić, M.; Zhen, B. Observation of bulk Fermi arc and polarization half charge from paired exceptional points. *Science* **2018**, *359*, 1009−1012.
(21) Berry, M. V. Quantal phase factors accompanying adiabatic changes. *Proc. R. Soc. London, Ser. A* **1984**, *392*, 45−57.
(22) Hernández, E.; Jáuregui, A.; Mondragón, A. Non-Hermitian degeneracy of two unbound states. *J. Phys. A: Math. Gen.* **2006**, *39*, 10087−10105.
(23) Heiss, W. Phases of wave functions and level repulsion. *Eur. Phys. J. D* **1999**, *7*, 1−4.
(24) Uzdin, R.; Mailybaev, A.; Moiseyev, N. On the observability and asymmetry of adiabatic state flips generated by exceptional points. *J. Phys. A: Math. Theor.* **2011**, *44*, 435302.
(25) Gilary, I.; Mailybaev, A. A.; Moiseyev, N. Time-asymmetric quantum-state-exchange mechanism. *Phys. Rev. A: At., Mol., Opt. Phys.* **2013**, *88*, No. 010102.
(26) Milburn, T. J.; Doppler, J.; Holmes, C. A.; Portolan, S.; Rotter, S.; Rabl, P. General description of quasiadiabatic dynamical phenomena near exceptional points. *Phys. Rev. A: At., Mol., Opt. Phys.* **2015**, *92*, 052124.
(27) von Neumann, J.; Wigner, E. P. Über das Verhalten von Eigenwerten bei adiabatischen Prozessen. *Phys. Z.* **1929**, *30*, 467.
(28) Teller, E. The Crossing of Potential Surfaces. *J. Phys. Chem.* **1937**, *41*, 109.
(29) Santra, R.; Cederbaum, L. S. Non-Hermitian electronic theory and applications to clusters. *Phys. Rep.* **2002**, *368*, 1−117.
(30) Mailybaev, A. A. Computation of multiple eigenvalues and generalized eigenvectors for matrices dependent on parameters. *Numer. Lin. Algebra Appl.* **2006**, *13*, 419−436.
(31) Cartarius, H.; Main, J.; Wunner, G. Exceptional points in the spectra of atoms in external fields. *Phys. Rev. A: At., Mol., Opt. Phys.* **2009**, *79*, 053408.
(32) Lefebvre, R.; Moiseyev, N. Localization of exceptional points with Padé approximants. *J. Phys. B: At., Mol. Opt. Phys.* **2010**, *43*, 095401.
(33) Uzdin, R.; Lefebvre, R. Finding and pinpointing exceptional points of an open quantum system. *J. Phys. B: At., Mol. Opt. Phys.* **2010**, *43*, 235004.
(34) Feldmaier, M.; Main, J.; Schweiner, F.; Cartarius, H.; Wunner, G. Rydberg systems in parallel electric and magnetic fields: an improved method for finding exceptional points. *J. Phys. B: At., Mol. Opt. Phys.* **2016**, *49*, 144002.
(35) Lefebvre, R.; Atabek, O.; Šindelka, M.; Moiseyev, N. Resonance Coalescence in Molecular Photodissociation. *Phys. Rev. Lett.* **2009**, *103*, 123003.
(36) Atabek, O.; Lefebvre, R.; Lepers, M.; Jaouadi, A.; Dulieu, O.; Kokoouline, V. Proposal for a Laser Control of Vibrational Cooling in Na_2Using Resonance Coalescence. *Phys. Rev. Lett.* **2011**, *106*, 173002.
(37) Kokoouline, V.; Wearne, A.; Lefebvre, R.; Atabek, O. Laser-controlled rotational cooling of Na_2 based on exceptional points. *Phys. Rev. A: At., Mol., Opt. Phys.* **2013**, *88*, 033408.
(38) Jaouadi, A.; Desouter-Lecomte, M.; Lefebvre, R.; Atabek, O. Signatures of exceptional points in the laser control of non-adiabatic vibrational transfer. *J. Phys. B: At., Mol. Opt. Phys.* **2013**, *46*, 145402.
(39) Zuev, D.; Jagau, T.-C.; Bravaya, K. B.; Epifanovsky, E.; Shao, Y.; Sundstrom, E.; Head-Gordon, M.; Krylov, A. I. Complex Absorbing Potentials within EOM-CC Family of Methods: Theory, Implementation, and Benchmarks. *J. Chem. Phys.* **2014**, *141*, 024102.
(40) Benda, Z.; Jagau, T.-C. Communication: Analytic Gradients for the Complex Absorbing Potential Equation-of-Motion Coupled-Cluster Method. *J. Chem. Phys.* **2017**, *146*, 031101.
(41) Because the crossing states mix when approaching the EP, the optimal parameters are also expected to become similar for the two states in the vicinity of the EP (at the exact EP, there is only one, self-orthogonal state, but this point is never reached in actual numerical calculations); thus, using the same set of parameters is not expected to cause large errors.
(42) Krylov, A. I. Equation-of-Motion Coupled-Cluster Methods for Open-Shell and Electronically Excited Species: The Hitchhiker's Guide to Fock Space. *Annu. Rev. Phys. Chem.* **2008**, *59*, 433−462.

DOI: 10.1021/acs.jpclett.8b03228
J. Phys. Chem. Lett. 2018, 9, 6978−6984

(43) Moiseyev, N.; Certain, P.; Weinhold, F. Resonance properties of complex-rotated hamiltonians. *Mol. Phys.* **1978**, *36*, 1613−1630.
(44) Hättig, C. In *Response Theory and Molecular Properties (A Tribute to Jan Linderberg and Poul Jørgensen)*; Jensen, H., Ed.; Advances in Quantum Chemistry; Academic Press, 2005; Vol. *50*, pp 37−60.
(45) Köhn, A.; Tajti, A. Can coupled-cluster theory treat conical intersections? *J. Chem. Phys.* **2007**, *127*, 044105.
(46) Kjønstad, E. F.; Myhre, R. H.; Martínez, T. J.; Koch, H. Crossing conditions in coupled cluster theory. *J. Chem. Phys.* **2017**, *147*, 164105.
(47) Kirillov, O. N.; Mailybaev, A. A.; Seyranian, A. P. Unfolding of eigenvalue surfaces near a diabolic point due to a complex perturbation. *J. Phys. A: Math. Gen.* **2005**, *38*, 5531−5546.
(48) van Langen, S. A.; Brouwer, P. W.; Beenakker, C. W. J. Fluctuating phase rigidity for a quantum chaotic system with partially broken time-reversal symmetry. *Phys. Rev. E: Stat. Phys., Plasmas, Fluids, Relat. Interdiscip. Top.* **1997**, *55*, R1−R4.
(49) Brouwer, P. W. Wave function statistics in open chaotic billiards. *Phys. Rev. E: Stat. Phys., Plasmas, Fluids, Relat. Interdiscip. Top.* **2003**, *68*, 046205.
(50) Bulgakov, E. N.; Rotter, I.; Sadreev, A. F. Phase rigidity and avoided level crossings in the complex energy plane. *Phys. Rev. E* **2006**, *74*, 056204.
(51) Rotter, I. A non-Hermitian Hamilton operator and the physics of open quantum systems. *J. Phys. A: Math. Theor.* **2009**, *42*, 153001.
(52) Bearpark, M. J.; Robb, M. A.; Schlegel, H. B. A direct method for the location of the lowest energy point on a potential surface crossing. *Chem. Phys. Lett.* **1994**, *223*, 269−274.
(53) Benda, Z.; Rickmeyer, K.; Jagau, T.-C. Structure Optimization of Temporary Anions. *J. Chem. Theory Comput.* **2018**, *14*, 3468−3478.
(54) Benda, Z.; Jagau, T.-C. Understanding Processes Following Resonant Electron Attachment: Minimum-Energy Crossing Points between Anionic and Neutral Potential Energy Surfaces. *J. Chem. Theory Comput.* **2018**, *14*, 4216−4223.
(55) Faraji, S.; Matsika, S.; Krylov, A. I. Calculations of non-adiabatic couplings within equation-of-motion coupled-cluster framework: Theory, implementation, and validation against multi-reference methods. *J. Chem. Phys.* **2018**, *148*, 044103.
(56) Shao, Y.; Gan, Z.; Epifanovsky, E.; Gilbert, A. T.; Wormit, M.; Kussmann, J.; Lange, A. W.; Behn, A.; Deng, J.; Feng, X.; et al. Advances in molecular quantum chemistry contained in the Q-Chem 4 program package. *Mol. Phys.* **2015**, *113*, 184−215.
(57) Epifanovsky, E.; Krylov, A. I. Direct location of the minimum point on intersection seams of potential energy surfaces with equation-of-motion coupled-cluster methods. *Mol. Phys.* **2007**, *105*, 2515−2525.
(58) The vicinity of an exceptional point affects the shape of the η trajectories, and the condition $\eta dE/d\eta$ = min.[67] no longer gives reliable η_{opt} values. The chosen value (9×10^{-3} a.u.) is slightly larger than η_{opt} of the $^2\Pi$ state at the neutral equilibrium structure (8.4×10^{-3} a.u.). Our investigations showed that using different CAP strength parameters affects the position of the EP line in parameter space, but if η is high enough, this change is small compared to the size of the area affected by the vicinity of the EP line. We discuss these properties in another article, and here we focus on the performance of the EP optimization algorithm instead.
(59) On a larger scale, the real degeneracy seam and imaginary degeneracy seam bend, but we were not able to verify whether they form a closed loop because of the limitations of the CAP-EOM-CCSD method to handle elongated bonds. The area affected by the EP seems to be rather large in parameter space, but this is not always the case as is apparent from the example of chloroethylene. We will present and discuss these interesting properties of HCN^- elsewhere, as they are not directly connected to the question of locating exceptional points.
(60) Sanche, L. Low energy electron-driven damage in biomolecules. *Eur. Phys. J. D* **2005**, *35*, 367−390.
(61) Johnson, J. P.; Christophorou, L. G.; Carter, J. G. Fragmentation of aliphatic chlorocarbons under low-energy ($\lesssim$ 10 eV) electron impact. *J. Chem. Phys.* **1977**, *67*, 2196−2215.
(62) Burrow, P. D.; Modelli, A.; Chiu, N. S.; Jordan, K. D. Temporary Σ and Π anions of the chloroethylenes and chlorofluoroethylenes. *Chem. Phys. Lett.* **1981**, *82*, 270−276.
(63) Kaufel, R.; Illenberger, E.; Baumgärtel, H. Formation and Dissociation of the Chloroethylene anions. *Chem. Phys. Lett.* **1984**, *106*, 342−346.
(64) Olthoff, J. K.; Tossell, J. A.; Moore, J. H. Electron attachment by haloalkenes and halobenzenes. *J. Chem. Phys.* **1985**, *83*, 5627−5634.
(65) Vasil'ev, Y. V.; Voinov, V. G.; Barofsky, D. F.; Deinzer, M. L. Absolute dissociative electron attachment cross-sections of chloro- and bromo-ethylenes. *Int. J. Mass Spectrom.* **2008**, *277*, 142−150.
(66) Carter, J. M.; Lapham, W. W.; Zogorski, J. S. Occurrence of Volatile Organic Compounds in Aquifers of the United States. *J. Am. Water Resour. Assoc.* **2008**, *44*, 399−416.
(67) Riss, U. V.; Meyer, H.-D. Calculation of Resonance Energies and Widths Using the Complex Absorbing Potential Method. *J. Phys. B: At., Mol. Opt. Phys.* **1993**, *26*, 4503−4536.

DOI: 10.1021/acs.jpclett.8b03228
J. Phys. Chem. Lett. 2018, 9, 6978−6984